MetAP2 inhibition increases energy expenditure through direct action on brown adipocytes

Received for publication, December 23, 2018, and in revised form, April 26, 2019 Published, Papers in Press, May 2, 2019, DOI 10.1074/jbc.RA118.007302

Huey-Jing Huang[‡1], Corine Holub[‡], Paul Rolzin[‡], James Bilakovics[‡], Andrea Fanjul[‡], Yoshinori Satomi[§], Artur Plonowski[‡], Christopher J. Larson[‡¶], and Pamela J. Farrell[‡]

From [‡]Takeda California, San Diego, California 92121, [§]Takeda Pharmaceutical Company Limited, Fujisawa 251-0012 Japan, and [¶]Sanford Burham Prebys Medical Discovery Institute, San Diego, California 92037

Edited by Jeffrey E. Pessin

Inhibitors of methionine aminopeptidase 2 (MetAP2) have been shown to reduce body weight in obese mice and humans. The target tissue and cellular mechanism of MetAP2 inhibitors, however, have not been extensively examined. Using compounds with diverse chemical scaffolds, we showed that MetAP2 inhibition decreases body weight and fat mass and increases lean mass in the obese mice but not in the lean mice. Obesity is associated with catecholamine resistance and blunted β-adrenergic receptor signaling activities, which could dampen lipolysis and energy expenditure resulting in weight gain. In the current study, we examined effect of MetAP2 inhibition on brown adipose tissue and brown adipocytes. Norepinephrine increases energy expenditure in brown adipose tissue by providing fatty acid substrate through lipolysis and by increasing expression of uncoupled protein-1 (UCP1). Metabolomic analysis shows that in response to MetAP2 inhibitor treatment, fatty acid metabolites in brown adipose tissue increase transiently and subsequently decrease to basal or below basal levels, suggesting an effect on fatty acid metabolism in this tissue. Treatment of brown adipocytes with MetAP2 inhibitors enhances norepinephrine-induced lipolysis and energy expenditure, and prolongs the activity of norepinephrine to increase ucp1 gene expression and energy expenditure in norepinephrine-desensitized brown adipocytes. In summary, we showed that the anti-obesity activity of MetAP2 inhibitors can be mediated, at least in part, through direct action on brown adipocytes by enhancing β-adrenergic–signaling–stimulated activities.

Inhibitors of methionine aminopeptidase 2 (MetAP2)[2] such as TNP-470 and fumagillin reduced body weight in ob/ob and high-fat diet–induced obese mice (1–4). Beloranib, a MetAP2 inhibitor from Zafgen, was shown to cause weight loss in obese humans (5–8), providing the clinical validation for targeting MetAP2-mediated pathway to treat obesity. Further development of beloranib was discontinued because of adverse effects, including its impact on thrombosis (6). Nevertheless, understanding the anti-obesity mechanisms of MetAP2 inhibition may facilitate future target/pathway selection and drug discovery.

MetAP2 gene and protein are widely expressed in many tissues, including liver, skeletal muscle, brain, and adipose tissue (The Human Protein Atlas, https://www.proteinatlas.org/ENSG00000111142-METAP2/tissue)[3] (26) and could potentially mediate the anti-obesity activity or adverse effect of MetAP2 inhibitor in these tissues. The anti-obesity effect of MetAP2 inhibition has been hypothesized to be at least partly through the adipose tissue. However, direct effect of MetAP2 inhibitors on adipose tissue and adipocytes has not been demonstrated. In humans, beloranib treatment increases plasma β-hydroxybutyrate, adiponectin, and FGF-21 levels and decreases fat mass and leptin levels, suggesting fatty acid metabolism and energy expenditure may be involved (8). In mice, MetAP2 inhibitor treatment increases energy expenditure in ob/ob and high-fat diet–induced obese mice (1, 2). Brown adipose tissue (BAT) is a thermogenic tissue important for regulating energy expenditure. Its presence in adult humans has been demonstrated and increasing BAT activity is proposed to be a promising obesity therapeutic approach (9). In the current study, we used MetAP2 inhibitors to probe the anti-obesity mechanism of MetAP2 inhibition, with a focus on brown adipose tissue and brown adipocytes.

Results

Use of chemically diverse MetAP2 compounds to probe the anti-obesity mechanism of MetAP2 inhibition

To understand the anti-obesity mechanism of MetAP2 inhibition, we used three MetAP2 inhibitors with different binding modes (reversible *versus* irreversible) and chemical scaffolds (Fig. 1*A*). Beloranib is a covalent, irreversible inhibitor from Zafgen and causes weight loss in humans (7). A357300 is a reversible inhibitor from Abbotts shown to have anti-tumor activity in animals but its anti-obesity activity has never been shown (10). Compound 1 is a novel reversible inhibitor from Takeda. Using three chemically different MetAP2 compounds increases the chance that the biological activities observed is because of MetAP2 inhibition and not compound-specific off-target effect.

The authors declare that they have no conflicts of interest with the contents of this article.

[1] To whom correspondence should be addressed. Tel.: 619-930-8217; E-mail: huey-jing.huang@takeda.com.

[2] The abbreviations used are: MetAP2, methionine aminopeptidase 2; BAT, brown adipose tissue; ALT, alanine transaminase; AST, aspartate transaminase; DIO, diet-induced obese; TCA, tricarboxylic acid; OCR, oxygen consumption rate; b.i.d., twice a day; sc, subcutaneously; q.d., every day; po, by mouth; AUC, area under the curve.

[3] Please note that the JBC is not responsible for the long-term archiving and maintenance of this site or any other third party hosted site.

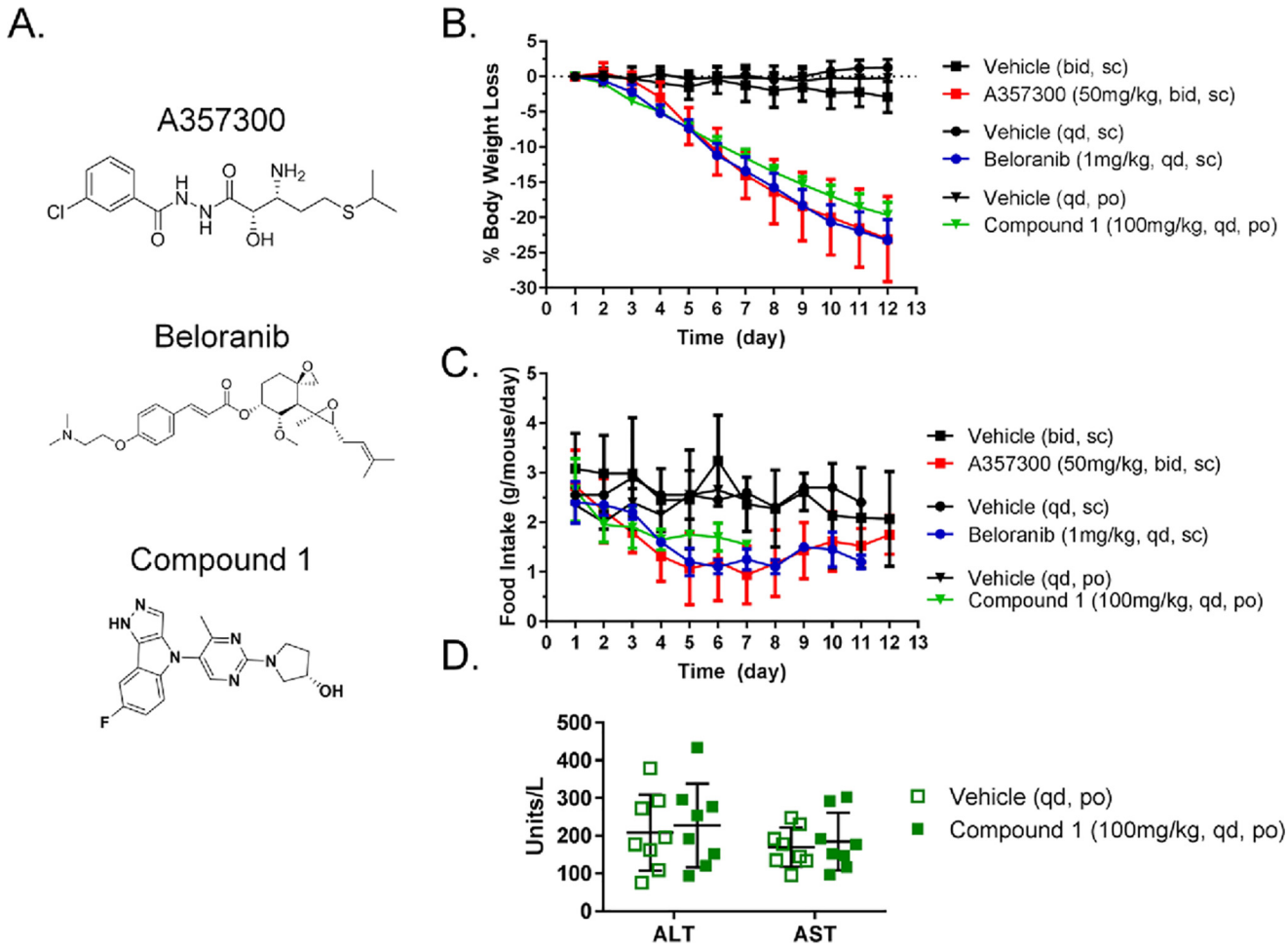

Figure 1. Three chemically diverse MetAP2 inhibitors reduce body weight and increase energy expenditure in high-fat diet–induced obese mice. *A*, chemical structures of MetAP2 inhibitors used in this study. *B*, male C57Bl/6 mice fed high-fat diet were treated with A35300 (50 mg/kg, b.i.d., sc), beloranib (1 mg/kg, q.d., sc), compound 1 (100 mg/kg, q.d., po), or vehicle. Body weight was measured every day. Data represent mean ± S.D., $n = 8$ per group except $n = 4$ for vehicle (q.d., sc) group. A357300-treated group: $p < 0.01$ *versus* vehicle (b.i.d., sc) on day 5, $p < 0.0001$ *versus* vehicle (b.i.d., sc) on days 6–12; beloranib-treated groups: $p < 0.0001$ *versus* vehicle (q.d., sc) on days 4–12; compound 1–treated group: $p < 0.001$ *versus* vehicle (q.d., po) on day 3, $p < 0.0001$ *versus* vehicle (q.d., po) on days 4–12 by two-way ANOVA, Bonferroni. *C*, food intake per cage (4 animals/cage) after 7–12 days of compound dosing was measured and shown as grams/mouse/day. Data represent mean ± S.D.; $n = 2$ cages (4 animals/cage) for vehicle (b.i.d., sc), A357300, vehicle (q.d., sc), beloranib; $n = 2$ cages (2–3 animals/cage) for vehicle (q.d., po), A357300 groups. *D*, plasma ALT and AST levels were measured after 12 days of treatment. Data represent mean ± S.D., $n = 8$ for vehicle and compound 1 groups.

All three MetAP2 inhibitors were first tested in high-fat diet–fed obese mice for their anti-obesity activities. Preliminary dose response experiments were conducted to select dose for each compound that causes similar weight loss (data not shown). As shown in Fig. 1*B*, all three compounds at the selected doses reduce body weight by 20–23% after 12 days of treatment. Food intake is in general reduced by MetAP2 inhibitor treatment within the first week of treatment but later normalized to the vehicle levels (Fig. 1*C*). To examine if there is tolerability issue with MetAP2 inhibitor treatment, the plasma alanine transaminase (ALT) and aspartate transaminase (AST) levels were measured. Elevation of these liver enzymes in the blood suggest liver damage. Fig. 1*D* shows that compound 1 did not affect ALT and AST levels after 12 days of MetAP2 inhibitor treatment.

MetAP2 inhibitors reduce body weight and adiposity in obese but not in lean mice

The effect of MetAP2 inhibitors to reduce body weight in obese mice is well-documented (1–4) but their effects on lean animals are less clear. To understand if the anti-obesity activity of MetAP2 inhibition is specific to the obese state, we compare the activities of MetAP2 compounds in high-fat diet–fed obese mice and normal chow-fed lean mice. Fig. 2 shows that at the doses selected, beloranib and compound 1 reduce body weight by 22–25% after 2 weeks of treatment in diet-induced obese (DIO) mice, but have minimal effect on body weight of lean mice.

High-fat diet feeding increases fat mass and decreases lean mass in mice as shown in Fig. 3. Beloranib and compound 1 at the doses selected reduce fat mass in obese mice but have no effect in the lean mice (Fig. 3, *A* and *C*). Similarly, both compounds increase lean mass in obese mice but have no effect on lean mass in the lean mice (Fig. 3, *B* and *D*).

The results from studies above show that the activities of MetAP2 inhibitors on body weight and fat accumulation are apparent in obese animals but not in lean animals. This suggests that the MetAP2 inhibition reduces body weight through selectively targeting the obese state to correct the defects associated with obesity.

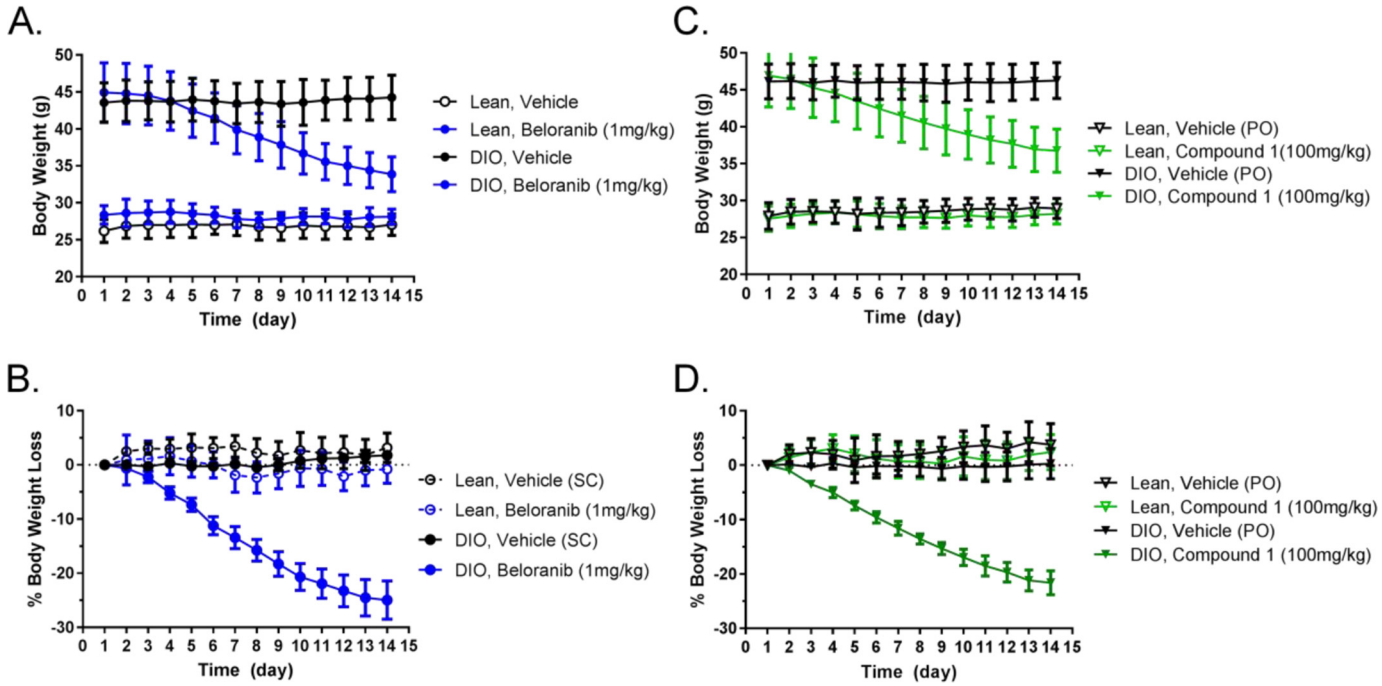

Figure 2. MetAP2 inhibitors reduce body weight in diet-induced obese mice, but not in lean mice. *A–D*, mice were fed with normal high fat diet (DIO) or normal chow (lean) and dosed with beloranib (1 mg/kg, q.d., sc) (*A* and *B*) or compound 1 (100 mg/kg, q.d., po) (*C* and *D*) for 14 days. Body weight was measured every day (*A* and *C*) and also expressed as change of body weight (*B* and *D*). Data represent mean ± S.D., $n = 8$ per group except $n = 4$ for lean, vehicle (sc) and DIO, vehicle (sc). DIO/Beloranib-treated group: $p < 0.0001$ vs DIO/Vehicle on days 4–14; Lean/Beloranib-treated group: $p < 0.05$ vs Lean/Vehicle on day 7; DIO/Compound1-treated group: $p < 0.0001$ vs DIO/Vehicle on days 4–14; Lean/Compound1-treated group: $p < 0.01$ vs Lean/Vehicle on day 3 by two-way ANOVA, Bonferroni.

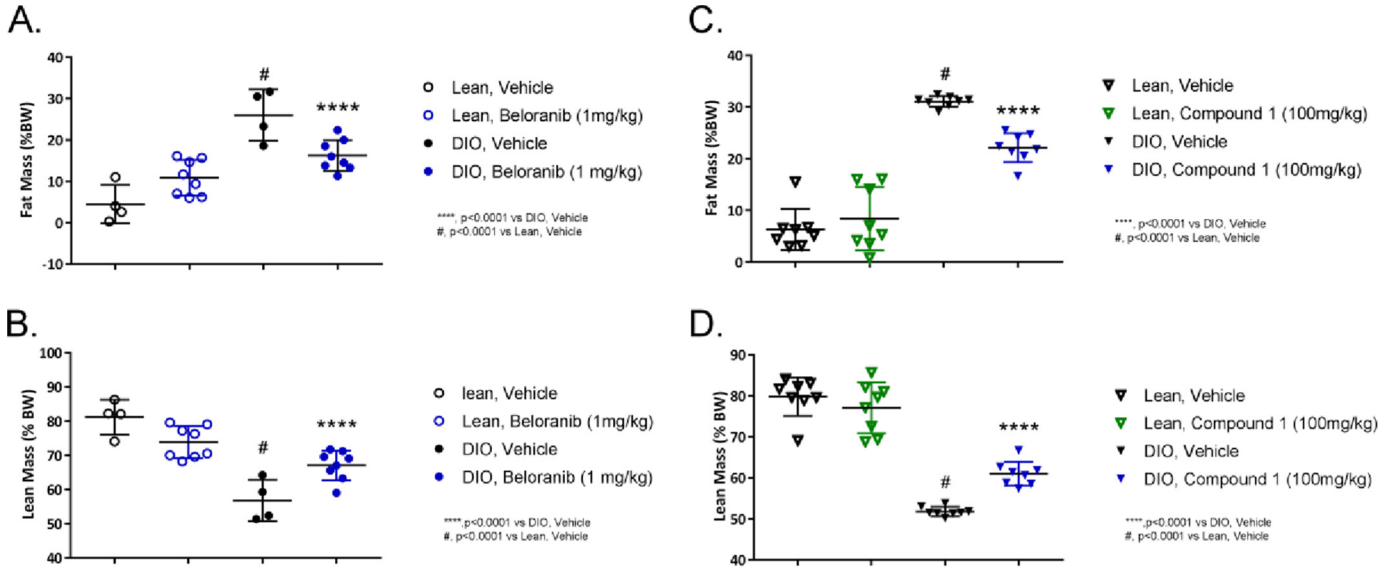

Figure 3. MetAP2 inhibitors reduce adiposity in obese but not in lean mice. *A–D*, mice were fed with normal high-fat diet (DIO) or normal chow (lean) and dosed with beloranib (*A* and *B*) or compound 1 (*C* and *D*) for 14 days, and fat and lean mass are measured expressed as % of total body weight. Data represent mean ± S.D., $n = 8$ per group except $n = 4$ for lean, vehicle (sc) and DIO, vehicle (sc) groups. #, $p < 0.05$ *versus* lean/vehicle, ****, $p < 0.0001$ *versus* DIO/vehicle by *t* test.

MetAP2 inhibitors affect fatty acid metabolism in brown adipose tissue of obese mice

To probe the mechanism of MetAP2 inhibition on brown adipose tissue, we chose to examine the metabolic profile of this tissue from obese mice that are treated with MetAP2 inhibitors for only 1 day. At this time point, body weight loss is not yet significant (see Figs. 1 and 2) so the metabolic change observed is more likely to be the cause and not the result of body weight loss. BAT was collected 2, 8, and 24 h post last dose to examine the dynamic metabolic changes after MetAP2 inhibitor treatment (Fig. 4*A*). To ensure MetAP2 target is engaged by the compounds, we measured the level of NMet-14–3-3γ. This is the N-terminal methionine-retained form of the MetAP2 substrate 14–3-3γ, the level of which can be detected using Western blot analysis (11). The NMet-14–3-3γ level is significantly increased by all three MetAP2 inhibitors at 2, 8, and 24 h, as

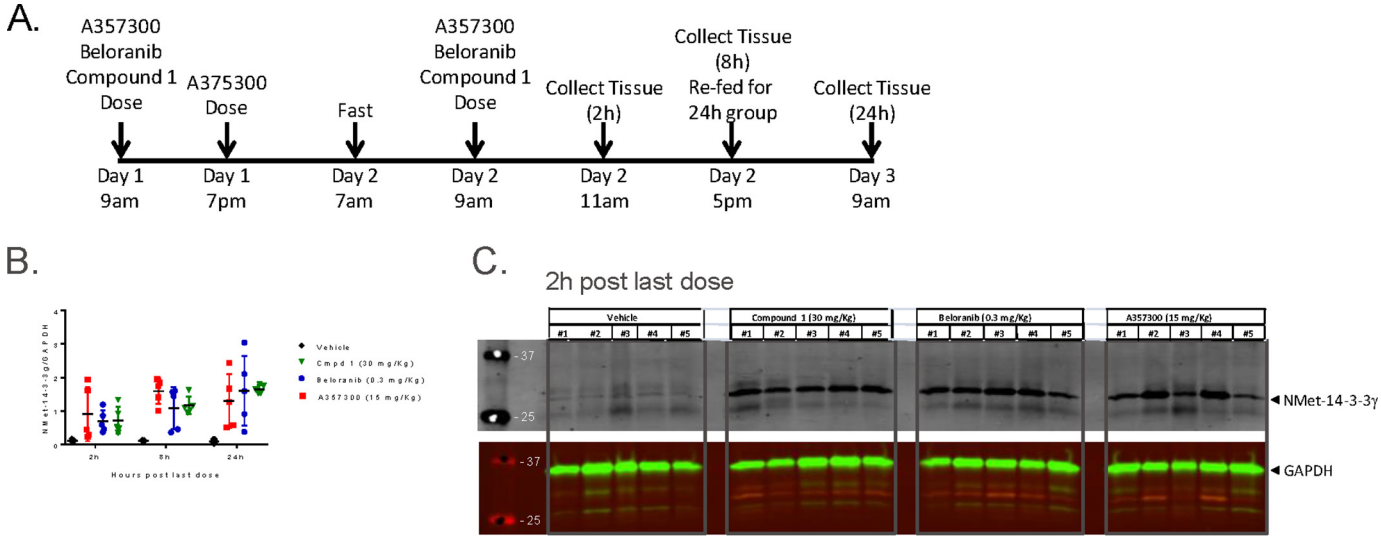

Figure 4. MetAP2 inhibitors decrease N-terminal cleavage of MetAP2 substrate 14–3-3γ in brown adipose of DIO obese mice. *A*, study design for metabolomic study. Mice fed with high-fat diet were dosed and tissues harvested as shown. *B*, Western blot analysis of NMet-14–3-3γ and GAPDH in brown adipose tissue protein extracts from mice dosed with vehicle or MetAP2 inhibitors. *C*, representative Western blotting images at 2 h post last dose were shown. Western blotting signals were quantified and shown as NMet-14–3-3γ/GAPDH ratio. Data represent mean ± S.D.; $n = 5$ per group.

shown in Fig. 4*B*. An example of NMet-14–3-3γ Western blotting at 2 h post dose is shown in Fig. 4*C*.

Metabolomic analysis of BAT shows that all three compounds significantly increased level of acylcarnitines of different lengths at the earliest time point 2 h (Fig. 5*A*). Acylcarnitines are intermediate oxidative metabolites that are generated for transporting long-chain fatty acids across mitochondrial membrane for β-oxidation. Increased acylcarnitine levels suggest mitochondrial fatty acid oxidation outpaces tricarboxylic acid (TCA) capacity (12); this could be because of mitochondrial dysfunction or excess increase of fatty acid oxidation rate. Interestingly, the increased acylcarnitine by MetAP2 inhibitor treatment at earlier time points was not sustained at later time points. Here most acylcarnitine species initially increased at 2 or 8 h and subsequently reduced to basal or below basal levels at 8 or 24 h (Fig. 5*A*). Similarly, free fatty acid levels in the BAT increased transiently at earlier time points and decreased at later time points (Fig. 5*B*). These results suggest that the observed increased acylcarnitine/free fatty acids may be more likely because of increased fatty acid flux into the BAT and not because of defect in mitochondrial fatty acid oxidation. The source of fatty acids may be from increased fatty acid uptake or increased lipolysis within the BAT after MetAP2 inhibitor treatment.

Metabolites in the sphingolipid biosynthesis pathway are similarly elevated at 2 and 8 h time points and most returned to basal levels at 24 h time point (Fig. 5*C*). These include ceramide,dihydroceramide,glucosylceramide/galactosylceramide, and sphingomyelin. Sphingolipids can be synthesized from acyl-CoA and serine. As suggested from the initial rise of acylcarnitines and free fatty acids (Fig. 5, *A–C*), there is a transient increase of fatty acid accumulation immediately after MetAP2 inhibitor treatment. These excess fatty acids may be shunted to sphingolipid biosynthesis pathway, resulting in transient increase of sphingolipids with MetAP2 inhibitor treatment.

MetAP2 inhibitors increase lipolysis and energy expenditure in primary brown adipocytes

The transient nature of increased fatty acid metabolites in the BAT suggest that there may be increased fatty acid uptake or lipolysis to provide fatty acid substrates for oxidation. Sympathetic activation of brown adipose tissue plays an important role in maintaining energy balance by stimulating lipolysis and energy expenditure (9). To explore the possibility that MetAP2 inhibition may directly enhance the sympathetic response of BAT, we tested the activity of MetAP2 inhibitors on brown adipocytes to increase lipolysis and energy expenditure in response to β-adrenergic agonists such as norepinephrine. In the absence of MetAP2 inhibitor treatment, norepinephrine increases lipolysis of brown adipocytes by 2-fold and this is measured by the glycerol levels released into the cell culture media (Fig. 6*A*). Treatment with MetAP2 inhibitors A357300, beloranib, or compound 1 significantly increases norepinephrine-induced glycerol release to 4- to 5-fold (Fig. 6*A*).

In response to norepinephrine treatment, brown adipocytes increase energy expenditure measured by oxygen consumption rate (OCR) using XF96 extracellular flux analyzer (Fig. 6*B*). Treatment with MetAP2 inhibitors A357300, beloranib, or compound 1 further enhances the ability of brown adipocytes to increase norepinephrine-induced OCR (Fig. 6*B*). These results suggest that MetAP2 inhibitors can enhance the β-adrenergic signaling pathway in brown adipocytes in a cell-autonomous manner.

MetAP2 inhibitor reverses norepinephrine desensitization in primary brown adipocytes

The *in vivo* data from Figs. 2 and 3 suggest that the anti-obesity activity of MetAP2 inhibitors selectively targets obese state. Obesity is associated with catecholamine resistance in adipose tissues (13–18). To mimic the catecholamine resistance in cells, we treated brown adipocytes with norepineph-

A.

Name	Fold change(v.s. vehicle)								
	2 hours			8 hours			24 hours		
	Compound 1	Beloranib	A357300	Compound 1	Beloranib	A357300	Compound 1	Beloranib	A357300
Acylcarnitine(C0)	1.6	1.3	1.5	0.6	1.3	1.2	0.7	0.9	1.1
Acylcarnitine(C2)	1.1	1.2	1.1	0.8	1.5	1.4	0.7	0.9	0.9
Acylcarnitine(C3)	1.7	1.3	1.4	0.5	1.3	1.3	0.8	1.1	1.1
Acylcarnitine(C4)	1.0	1.4	1.1	0.8	1.4	1.3	0.8	0.9	1.2
Acylcarnitine(C4OH)	1.4	1.3	1.1	0.7	1.1	1.3	0.7	0.9	0.9
Acylcarnitine(C5)	0.9	1.2	1.1	0.8	1.6	1.0	0.7	0.8	0.9
Acylcarnitine(C5OH)	1.6	1.6	1.9	0.7	1.1	1.4	0.7	1.4	1.2
Acylcarnitine(C6)	0.9	1.4	1.1	0.6	1.3	1.1	0.5	0.7	0.8
Acylcarnitine(C6OH)	2.4	2.1	1.1	0.4	1.1	1.2	1.0	0.8	2.2
Acylcarnitine(C8)	1.2	1.4	1.4	0.6	1.4	1.1	0.5	0.8	0.8
Acylcarnitine(C10)	1.3	1.2	1.5	0.6	1.4	1.1	0.6	1.0	0.9
Acylcarnitine(C12)	1.1	1.2	1.1	0.6	1.1	1.0	0.6	0.9	0.8
Acylcarnitine(C14)	1.0	1.0	1.0	0.8	1.1	0.9	0.7	0.9	0.9
Acylcarnitine(C16)	0.9	1.1	1.1	0.7	1.1	0.8	0.7	0.9	0.9
Acylcarnitine(C16:1)	0.8	1.0	1.1	0.7	1.0	0.8	0.7	1.0	0.8
Acylcarnitine(C16OH)	1.2	0.9	1.0	0.8	0.9	0.7	0.9	1.2	1.0
Acylcarnitine(C18)	1.0	1.1	1.3	0.6	1.2	1.0	0.6	0.9	0.7
Acylcarnitine(C18:1)	1.0	1.1	1.2	0.7	1.1	0.8	0.6	0.9	0.8
Acylcarnitine(C18:2)	1.0	1.1	1.3	0.6	1.1	0.8	0.6	0.9	0.8
Acylcarnitine(C18:3)	1.1	1.4	1.5	0.7	1.0	0.7	0.6	0.9	0.7
Acylcarnitine(C20:4)	1.0	1.7	1.3	0.9	1.4	0.9	0.8	1.2	1.3

Fold change<1	p>=0.1	0.5
	p<0.1	0.5
	p<0.05	0.5
	p<0.01	0.5
	p<0.001	0.6
Fold change>1	p>=0.1	2.0
	p<0.1	2.0
	p<0.05	2.0
	p<0.01	2.0
	p<0.001	2.0

B.

Name	Fold change(v.s. vehicle)								
	2 hours			8 hours			24 hours		
	Compound 1	Beloranib	A357300	Compound 1	Beloranib	A357300	Compound 1	Beloranib	A357300
Free fatty acid (C14:0)	1.4	1.0	1.0	0.8	0.8	0.8	0.8	0.8	1.0
Free fatty acid (C14:1)	1.4	0.9	0.9	0.9	0.7	0.9	0.8	0.9	1.0
Free fatty acid (C16:0)	1.7	1.1	1.2	0.7	0.9	0.9	0.8	0.7	1.0
Free fatty acid (C16:1)	1.5	0.9	1.0	0.8	0.8	0.9	0.8	0.8	1.1
Free fatty acid (C16:2)	2.2	1.1	1.4	0.4	0.8	1.0	0.7	0.8	1.0
Free fatty acid (C17:0)	1.9	1.1	1.3	0.6	0.9	1.0	0.8	0.7	1.0
Free fatty acid (C17:1)	1.8	1.0	1.1	0.6	0.8	1.0	0.8	0.7	1.0
Free fatty acid (C18:0)	1.5	1.2	1.2	0.7	1.0	1.0	0.8	0.8	0.9
Free fatty acid (C18:1)	1.7	1.0	1.2	0.7	1.0	1.1	0.8	0.7	1.0
Free fatty acid (C18:2)	1.8	1.0	1.3	0.6	0.9	1.0	0.8	0.8	1.0
Free fatty acid (C18:3)	1.9	1.1	1.2	0.6	0.8	0.8	0.7	0.7	1.0
Free fatty acid (C20:1)	1.7	1.1	1.2	0.7	0.9	1.1	0.7	0.7	0.9
Free fatty acid (C20:2)	1.7	1.1	1.3	0.6	0.9	1.0	0.8	0.9	1.1
Free fatty acid (C20:3)	1.6	1.1	1.2	0.7	0.8	0.9	0.9	1.1	1.2
Free fatty acid (C20:4)	1.4	1.1	1.1	0.8	1.1	1.1	1.0	1.2	1.2
Free fatty acid (C20:5)	1.5	1.0	1.2	0.7	0.7	1.1	0.8	1.0	1.1
Free fatty acid (C20:5)	0.7	0.9	0.8	0.7	0.7	1.5	0.9	1.3	1.0
Free fatty acid (C22:0)	1.3	1.2	1.3	1.7	1.2	1.4	0.8	0.8	0.8
Free fatty acid (C22:1)	1.4	1.1	1.2	0.9	1.1	1.3	0.6	0.6	0.8
Free fatty acid (C22:2)	1.4	1.1	1.2	0.8	1.0	1.2	0.7	0.8	1.1
Free fatty acid (C22:3)	1.7	1.2	1.4	0.7	0.9	1.0	0.8	1.1	1.4
Free fatty acid (C22:4)	1.4	1.3	1.5	0.8	0.9	1.0	0.9	1.2	1.4
Free fatty acid (C22:5)	1.4	1.3	1.6	0.7	0.9	1.0	1.0	1.3	1.5
Free fatty acid (C22:6)	1.3	1.3	1.4	0.7	1.0	1.3	0.9	1.3	1.3
Free fatty acid (C24:0)	1.1	1.1	1.1	1.6	1.2	1.3	1.0	0.9	1.0
Free fatty acid (C24:1)	1.2	1.2	1.3	2.0	1.3	1.6	0.7	0.8	0.9
Free fatty acid (C24:2)	1.1	1.3	1.5	2.0	1.2	1.9	0.9	0.8	1.3
Free fatty acid (C24:4)	1.3	1.3	1.3	0.9	1.2	1.5	0.7	1.2	1.6
Free fatty acid (C24:5)	1.6	1.3	1.4	0.7	1.0	0.9	0.7	1.1	1.6
Free fatty acid (C24:6)	1.5	1.2	1.2	0.6	0.9	0.9	1.1	1.4	2.2
Free fatty acid (C26:0)	0.8	1.1	1.1	1.6	1.0	1.2	1.2	1.2	1.2

C.

Name	Fold change(v.s. vehicle)								
	2 hours			8 hours			24 hours		
	Compound 1	Beloranib	A357300	Compound 1	Beloranib	A357300	Compound 1	Beloranib	A357300
Ceramide(14:0)	0.9	1.4	1.0	2.0	0.7	1.0	1.2	0.9	1.1
Ceramide(16:0)	0.9	1.4	1.2	2.3	1.1	1.8	1.6	1.4	1.4
Ceramide(16:1)	1.0	1.3	1.0	1.9	1.0	1.5	1.2	1.3	1.1
Ceramide(17:0)	0.6	1.2	1.2	0.9	0.9	0.8	0.9	1.0	0.8
Ceramide(18:0)	0.6	1.2	1.0	0.9	1.0	0.8	1.0	1.0	0.9
Ceramide(18:1)	0.6	1.1	0.9	1.1	1.0	0.9	1.1	1.1	1.0
Ceramide(18:2)	0.7	1.1	1.1	1.2	0.9	1.0	1.4	1.4	2.0
Ceramide(19:0)	1.3	1.5	1.6	1.0	0.9	1.1	1.5	1.2	1.2
Ceramide(20:0)	1.1	1.3	1.3	1.1	1.0	1.1	1.2	1.1	1.4
Ceramide(20:1)	0.6	0.9	0.8	1.7	0.8	1.0	1.7	1.5	1.5
Ceramide(21:0)	1.4	1.4	1.4	1.2	1.1	1.2	1.2	0.9	1.2
Ceramide(22:0)	1.3	1.4	1.4	1.2	1.1	1.1	1.2	1.1	1.4
Ceramide(22:1)	0.8	1.2	1.0	1.5	1.0	1.0	1.4	1.2	1.2
Ceramide(22:2)	0.6	1.0	0.9	2.4	0.7	1.4	2.2	1.6	1.3
Ceramide(23:0)	1.3	1.3	1.4	1.0	1.3	1.1	1.2	1.1	1.3
Ceramide(23:1)	0.9	1.1	1.0	1.3	1.1	1.0	1.3	1.1	1.1
Ceramide(24:0)	1.3	1.4	1.4	1.0	1.3	1.2	1.1	1.0	1.2
Ceramide(24:1)	1.2	1.2	1.2	1.3	1.1	1.1	1.2	1.0	1.1
Ceramide(24:2)	1.0	1.2	1.0	1.5	1.1	1.1	1.3	1.1	1.1
Ceramide(24:3)	0.8	1.2	0.9	1.9	0.8	1.2	1.8	1.4	1.0
Ceramide(25:0)	1.4	1.2	1.5	0.9	1.5	1.3	1.1	1.1	1.2
Ceramide(25:1)	1.1	1.2	1.2	1.2	1.3	1.2	1.4	1.2	1.3
Ceramide(26:1)	1.2	1.3	1.5	1.4	2.0	1.6	1.2	1.2	1.1
Dihydroceramide(14:0)	2.1	2.1	2.1	1.9	1.5	1.8	1.1	1.1	1.3
Dihydroceramide(15:0)	0.9	1.7	1.6	2.7	0.5	1.9	1.9	2.0	1.5
Dihydroceramide(16:0)	0.8	1.4	1.3	2.2	0.9	1.8	1.3	1.2	1.2
Dihydroceramide(18:0)	0.9	1.3	1.2	1.4	1.3	1.3	1.2	1.0	1.1
Dihydroceramide(20:0)	0.9	1.4	1.4	1.3	2.6	1.4	1.6	1.2	1.6
Dihydroceramide(22:0)	1.2	1.3	1.3	1.3	1.1	1.1	1.1	0.9	1.2
Dihydroceramide(23:0)	1.1	1.4	1.4	1.3	1.1	1.0	1.1	0.8	1.1
Dihydroceramide(24:0)	1.2	1.5	1.8	1.1	0.9	1.0	1.2	0.7	1.0
Dihydroceramide(25:0)	0.7	1.0	1.1	1.1	1.0	1.2	1.8	1.4	1.7
Glc/Gal-ceramide(16:0)	1.0	1.5	1.3	2.6	0.8	1.8	1.4	1.3	1.3
Glc/Gal-ceramide(18:0)	1.3	1.0	1.2	0.7	1.0	0.8	0.8	0.8	0.8
Glc/Gal-ceramide(20:0)	1.4	1.0	1.3	1.0	0.9	0.8	1.0	0.8	1.0
Glc/Gal-ceramide(21:0)	2.2	2.3	2.1	0.8	0.7	1.4	0.8	0.8	1.0
Glc/Gal-ceramide(22:0)	1.4	1.2	1.5	1.0	1.0	1.2	0.9	0.9	1.1
Glc/Gal-ceramide(22:1)	1.4	1.2	1.2	0.9	0.8	0.7	0.8	0.8	0.6
Glc/Gal-ceramide(23:0)	1.5	1.1	1.4	0.8	1.1	1.1	0.9	0.9	1.1
Glc/Gal-ceramide(24:0)	1.5	1.0	1.4	0.8	1.0	0.9	0.9	0.8	1.1
Glc/Gal-ceramide(24:1)	1.4	1.1	1.3	0.7	1.0	0.9	0.8	0.8	0.9
Glc/Gal-ceramide(24:2)	1.2	1.0	1.3	0.7	1.0	0.8	0.7	0.8	0.8
Sphingomyelin(14:0)	1.1	1.2	1.2	1.3	1.1	1.3	1.1	1.0	1.2
Sphingomyelin(16:0)	1.1	1.2	1.1	1.1	1.2	1.2	1.0	1.0	1.0
Sphingomyelin(16:1)	1.0	1.0	1.0	1.1	1.1	1.2	0.9	1.0	0.8
Sphingomyelin(18:0)	1.0	1.1	1.1	0.8	1.1	1.1	0.9	1.0	1.0
Sphingomyelin(18:1)	0.9	1.0	1.0	1.2	1.1	1.2	1.1	1.3	1.1
Sphingomyelin(18:2)	0.9	1.0	1.4	1.1	1.2	1.6	1.1	1.8	1.1
Sphingomyelin(20:0)	1.1	1.1	1.2	0.8	1.1	1.1	1.0	1.0	1.0
Sphingomyelin(20:1)	0.9	0.8	0.9	1.2	1.1	1.3	1.2	1.2	1.1
Sphingomyelin(22:0)	1.3	1.2	1.3	0.9	1.2	1.1	0.9	0.9	1.0
Sphingomyelin(22:1)	1.0	1.1	1.1	1.2	1.0	1.2	1.1	1.1	1.1
Sphingomyelin(24:0)	1.4	1.3	1.4	0.8	1.3	1.2	0.8	0.8	1.0
Sphingomyelin(24:1)	1.3	1.2	1.2	0.9	1.1	1.1	0.8	0.9	1.0
Sphingomyelin(24:2)	1.1	1.2	1.1	1.2	1.0	1.2	1.0	1.0	1.0

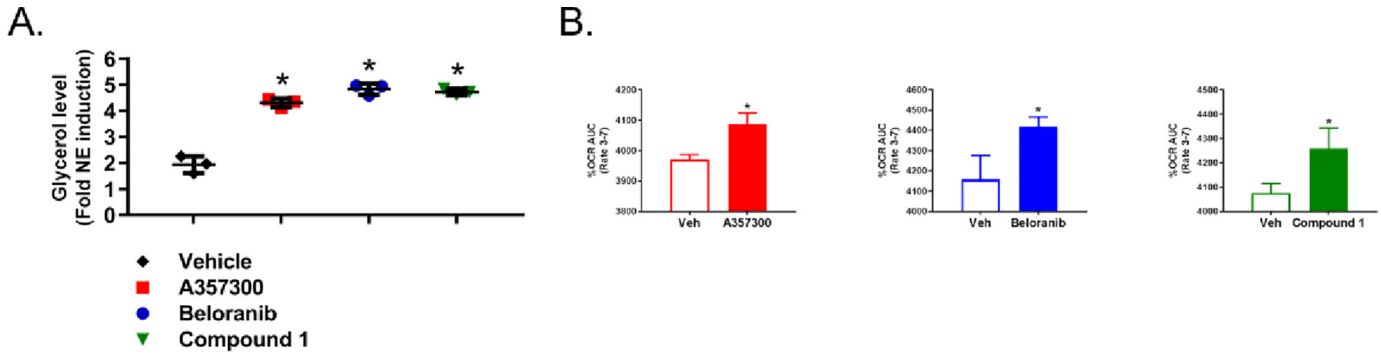

Figure 6. MetAP2 inhibitors increase norepinephrine-induced lipolysis and energy expenditure in primary brown adipocytes. Primary rat brown adipocytes were pretreated with MetAP2 compounds for 24 h followed by 3 h of norepinephrine (1 μM) treatment. *A*, lipolysis is assessed by release of glycerol into the culture medium and represented as -fold change compared with vehicle during 3 h of compound + norepinephrine treatment. Data represent mean ± S.D., $n = 3$ per group. *B*, energy expenditure is assessed by OCR and represented as area under the curve (AUC) after norepinephrine addition. Data represent mean ± S.D., $n = 4$ per group. *, $p < 0.05$ *versus* vehicle by *t* test.

rine for 24 h. In the absence of norepinephrine pretreatment, addition of norepinephrine induces an acute 30% increase of OCR followed by desensitization of this response (Fig. 7*A*, *light blue line*). Pretreatment with norepinephrine significantly dampens the norepinephrine-induced OCR (Fig. 7*A*, *dark blue line*), indicating that the cells become resistant to norepinephrine effect. Importantly, brown adipocytes treated with MetAP2 inhibitor A357300 have sustained OCR increase that does not become desensitized (Fig. 7*B*, *red line*) when compared with those treated with vehicle only (Fig. 7*B*, *dark blue line*).

Uncoupling protein 1 (UCP1) is the specific marker of BAT and transcriptionally activated in response to sympathetic stimulation (19). Treatment of brown adipocytes with norepinephrine increases ucp1 gene expression maximally at 5 h and this response decreases significantly after 24 h, suggesting a feedback regulation and desensitization (Fig. 7*C*). In Fig. 7*D*, brown adipocytes treated with norepinephrine (1 μM) increase ucp1 gene expression by 124-fold at 4 h but decrease to 31-fold at 24 h. Pretreatment with A357300 or beloranib can increase the ucp1 expression to 88-fold and 177-fold, respectively, at 24 h. These results suggest that MetAP2 inhibition can maintain ucp1 up-regulation after prolonged norepinephrine treatment (Fig. 7*D*).

Overall these results suggest that anti-obesity activity of MetAP2 inhibitors may be at least in part because of overcoming the catecholamine resistance of brown adipocytes, leading to enhanced energy expenditure and ucp1 gene expression.

Discussion

The weight reduction by MetAP2 inhibitor beloranib in obese humans is significant and robust. Understanding of the anti-obesity mechanism of MetAP2 inhibition may provide further insight of future target/pathway selection for obesity therapeutics. In the current study we showed that the anti-obesity effect of MetAP2 inhibitors is more pronounced in the obese animals, suggesting that MetAP2 inhibition may correct obesity-associated defects such as catecholamine resistance. Consistent with this hypothesis, MetAP2 inhibition reversed norepinephrine-induced resistance on energy expenditure and Ucp1 gene expression in brown adipocytes. To our knowledge, the effects of MetAP2 inhibition on BAT and brown adipocytes have not been explored previously. Here we show that MetAP2 inhibitors affect fatty acid metabolism in brown adipose and this could be mediated directly through brown adipocytes by enhancing norepinephrine-induced lipolysis and energy expenditure.

The metabolomic analysis of the brown adipose tissue treated by MetAP2 inhibitors shows increase of free fatty acids, acylcarnitines, and sphingolipids such as ceramide that are associated with lipotoxicity (20). For example, increased adipocyte sphingolipids by overnutrition is shown to reduce energy expenditure (21). However, in the current study the effect of MetAP2 inhibition on BAT fatty acid metabolism is dynamic, with immediate increase of fatty acid metabolites after compound treatment, followed by their decrease to the vehicle levels or lower after 24-h treatment. This suggests that increase of fatty acid influx followed by fatty acid oxidation is likely the mechanism of MetAP2 inhibitor and underscores the importance of a time-course study to track the metabolic flux to provide a more global picture of effect of MetAP2 inhibition. The consistent directions of change in many metabolites involved in fatty acid metabolism (free fatty acids, acylcarnitines, sphingolipids), and with three chemically diverse compounds strongly suggest that MetAP2 inhibitors have an impact on fatty acid metabolism. The metabolites identified from this study potentially can be used as biomarkers in the clinical setting.

It is unclear how inhibition of a methionine aminopeptidase can regulate fatty acid metabolism. MetAP2 cleaves the N-terminal methionine from newly synthesized protein. The free methionine released by MetAP2, if reaching significant value in cells, potentially could affect cellular functions that are impacted by methionine metabolism. Interestingly, methionine restriction was shown to reduce body weight and adiposity, and increase energy expenditure (22–24). In addition to being a substrate for protein synthesis, methionine can enter into various metabolic pathways. Activation of methionine to

Figure 5. MetAP2 inhibitors affect fatty acid metabolism in brown adipose of DIO obese mice. Mice were dosed with MetAP2 compounds and brown adipose tissues were harvested for metabolomic analysis. *A–C*, the metabolomic data are presented as -fold change as compared with vehicle. *Red* indicates a significant increase, and *blue* indicates a significant decrease in the level of metabolites as compared with vehicle.

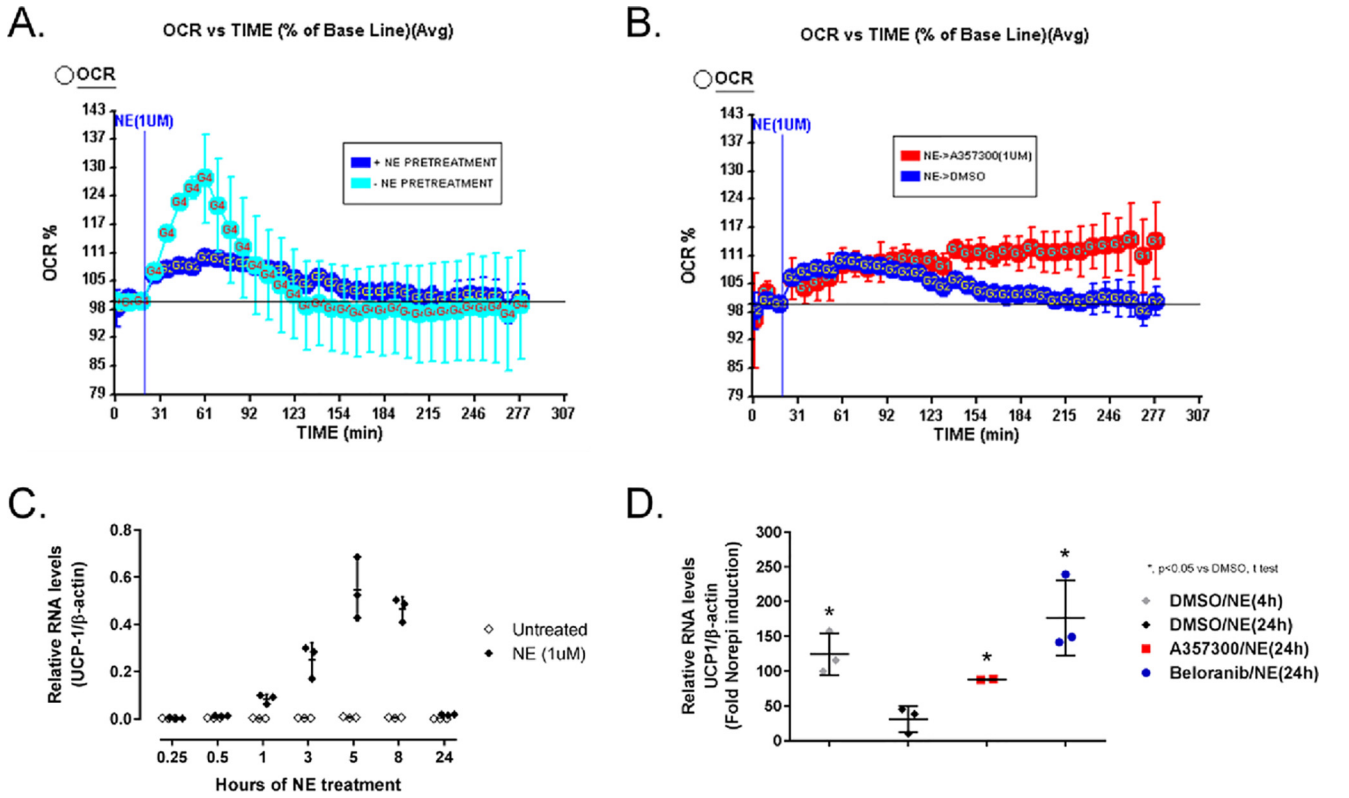

Figure 7. MetAP2 inhibitor reverses norepinephrine desensitization in brown adipocytes. *A*, norepinephrine desensitization is induced by pretreatment of primary rat brown adipocytes with norepinephrine (1 μM) for 24 h. *Blue line* indicates when fresh norepinephrine (*NE*) 1 μM is added. Data are presented as % of OCR when NE is injected. *B*, brown adipocytes pretreated with NE (1uM) and compound for 24 h followed by fresh NE injection at the *blue line*. *C*, brown adipocytes are treated with or without NE (1 μM) for the indicated time, and RNA are isolated for RT-qPCR analysis. *D*, brown adipocytes are treated with NE for 4 h (*gray*) or 24 h with vehicle (*black*) or with MetAP2 inhibitors (*red* and *green*). Data represent mean ± S.D., $n = 4$ per group. *, $p < 0.05$ *versus* vehicle by *t* test.

S-adenosylmethionine, the universal methyl donor for DNA, mRNA, and histone methylation, could lead to altered expression of genes involved in lipid metabolism and energy expenditure (25).

The effect of MetAP2 inhibitors on body weight does not appear to be because of its adverse effect. First, although the food intake is reduced in the first week of treatment, this is consistently normalized to vehicle levels afterward. The food intake effect of MetAP2 inhibitor is also consistent with the inhibition of hyperphasia in obese humans by beloranib treatment (6). Second, the plasma levels of liver enzymes AST and ALT are not affected by MetAP2 inhibitor treatment, suggesting that there is no hepatotoxicity with MetAP2 inhibitor. Third, the reduced body weight by MetAP2 inhibitors is not observed in the lean animals, suggesting that there is no general tolerability issue with MetAP2 inhibition. In summary, we have shown that one mechanism that the MetAP2 inhibitors cause body weight loss could be through correcting obesity defects such as catecholamine resistance in brown adipocytes. These data demonstrate the direct effect of MetAP2 inhibitors on brown adipose tissue and adipocytes, and contribute to further understanding of obesity biology and anti-obesity activity of MetAP2 inhibition.

Experimental procedures

Materials, reagents, and antibodies

Beloranib, A357300, and compound 1 were synthesized at Takeda California (San Diego, CA). Norepinephrine was purchased from Sigma. NMet14–3-3γ antibody was purchased from Novus Biologicals (Littleton, CO). GAPDH antibody was purchased from United States Biological (Salem, MA).

Animals

All animal studies were approved by the Takeda California Institutional Animal Care and Use Committee (IACUC). C57BL/6 mice at 6- to 8-weeks old were obtained from Jackson Laboratory and fed a 60% fat diet (HDF, Research Diet D12492) or normal chow diet for ~20 weeks. Mice were 26- to 33-weeks old at the start of the study. Body composition was determined by NMR imaging analysis. At the end of study, mice were euthanized by CO_2 inhalation.

Metabolomic analysis

Methanol (LC/MS grade), ethanol (HPLC grade), isopropanol (LC/MS grade), and 2 mol/liter ammonia isopropanol solution, 0.2 M disodium dihydrogen EDTA-2Na solution were purchased from Wako Pure Chemical (Osaka, Japan). All lipid standards were purchased from Avanti Polar Lipids (Alabaster, AL), Sigma-Aldrich, Wako Pure Chemical (Osaka, Japan), Tokyo Chemical Industry (Tokyo, Japan), Larodan Fine Chemicals (Malmö, Sweden), and MP Biomedicals (Santa Ana, CA). Tissue was homogenized in isopropanol (100 mg/ml) for lipidomics or in methanol (100 mg/ml) for GC/MS and IP-LC/MS/MS by a ShakeMaster Auto machine (BioMedical Science, Tokyo, Japan), and centrifuged at 15,000 rpm for 5 min. The

supernatant was applied to each metabolomic analysis. For lipidomic analysis, each 5-μl sample was injected onto a CAPCELL PAK ADME column (2.1 × 100 mm, 2.7 μm, Shiseido, Kyoto, Japan) and maintained at 60 °C. Chromatographic separation was performed by gradient elution of mobile phase A, 0.01% acetic acid, 1 mM ammonia and 10 μM EDTA-2Na in MilliQ water, and mobile phase B, 0.001% acetic acid and 0.2 mM ammonia in ethanol/isopropanol (1:1), with flow rate at 0.7 ml/min. Mass spectrometry analysis was performed using a Orbitrap XL mass spectrometer (Thermo Fisher Scientific) by both positive and negative ionization mode separately.

Brown adipocyte culture

Primary rat brown pre-adipocytes were purchased from Cosmo Bio Co., LTD, Tokyo, Japan (catalogue no. PMC-BAT10-COS). For measuring OCR using XF96 analyzer, primary rat brown pre-adipocytes were seeded at 10,000 cells/well in growth medium (PMC-BATGM-COS, Cosmo Bio Co., LTD, Japan) in XF96 cell plate (Seahorse Biosciences, North Billerica, MA) and incubated at 37 °C under 5% CO_2 for 1 day. Next day, medium was changed to differentiation medium (PMC-BATDM-COS, Cosmo Bio Co., LTD, Japan). After 2 days in differentiation medium, medium was changed to maintenance medium (PMC-BATMM-COS, Cosmo Bio Co., LTD, Japan). Cells were allowed to differentiate in the maintenance medium for 5 days with medium change every 2–3 days before experiment.

Oxygen consumption rate measurement

OCR measurements were performed using the XF96 Extracellular Flux analyzer (Seahorse Bioscience, North Billerica, MA). Prior to performing an assay, cells were washed with XF assay buffer (XF Assay medium, 25 mM glucose, 2 mM sodium pyruvate, pH7.4). A final volume of 175 μl of XF assay buffer was added and cells were transferred to a 37 °C incubator not supplemented with CO_2 (XF96 Prep Station) for 1 h before start of an assay. Each measurement cycle consisted of a mixing time of 3 min and a measuring time of 3 min. Norepinephrine was prepared at 8× concentration and 25 μl was added to each injection port for a final norepinephrine concentration of 1 μM in the measurement cycle. Four baseline measurements were taken and six response measurements were taken after addition of norepinephrine. OCR was normalized to protein content and reported as basal OCR, percentage of the baseline oxygen consumption (OCR %), or area under the curve (AUC) of the %OCR in response to norepinephrine (%OCR AUC).

Author contributions—H.-J. H. conceptualization; H.-J. H., C. J. L., and P. J. F. resources; H.-J. H., C. H., P. R., J. B., A. F., Y. S., and A. P. data curation; H.-J. H. software; H.-J. H., C. H., A. F., Y. S., and A. P. formal analysis; H.-J. H., A. P., C. J. L., and P. J. F. supervision; H.-J. H., C. J. L., and P. J. F. funding acquisition; H.-J. H., C. H., A. F., and Y. S. validation; H.-J. H. investigation; H.-J. H., C. H., A. F., and Y. S. visualization; H.-J. H., A. F., and Y. S. methodology; H.-J. H. writing-original draft; H.-J. H. project administration; H.-J. H. writing-review and editing.

References

1. Rupnick, M. A., Panigrahy, D., Zhang, C. Y., Dallabrida, S. M., Lowell, B. B., Langer, R., and Folkman, M. J. (2002) Adipose tissue mass can be regulated through the vasculature. *Proc. Natl. Acad. Sci. U.S.A.* **99,** 10730–10735 CrossRef Medline
2. White, H. M., Acton, A. J., and Considine, R. V. (2012) The angiogenic inhibitor TNP-470 decreases caloric intake and weight gain in high-fat fed mice. *Obesity* **20,** 2003–2009 CrossRef Medline
3. Lijnen, H. R., Frederix, L., and Van Hoef, B. (2010) Fumagillin reduces adipose tissue formation in murine models of nutritionally induced obesity. *Obesity* **18,** 2241–2246 CrossRef Medline
4. Bråkenhielm, E., Cao, R., Gao, B., Angelin, B., Cannon, B., Parini, P., and Cao, Y. (2004) Angiogenesis inhibitor, TNP-470, prevents diet-induced and genetic obesity in mice. *Circulation Res.* **94,** 1579–1588 CrossRef Medline
5. Shoemaker, A., Proietto, J., Abuzzahab, M. J., Markovic, T., Malloy, J., and Kim, D. D. (2017) A randomized, placebo-controlled trial of beloranib for the treatment of hypothalamic injury-associated obesity. *Diabetes Obes. Metab.* **19,** 1165–1170 CrossRef Medline
6. McCandless, S. E., Yanovski, J. A., Miller, J., Fu, C., Bird, L. M., Salehi, P., Chan, C. L., Stafford, D., Abuzzahab, M. J., Viskochil, D., Barlow, S. E., Angulo, M., Myers, S. E., Whitman, B. Y., Styne, D., *et al.* (2017) Effects of MetAP2 inhibition on hyperphagia and body weight in Prader-Willi syndrome: A randomized, double-blind, placebo-controlled trial. *Diabetes Obes. Metab.* **19,** 1751–1761 CrossRef Medline
7. Kim, D. D., Krishnarajah, J., Lillioja, S., de Looze, F., Marjason, J., Proietto, J., Shakib, S., Stuckey, B. G., Vath, J. E., and Hughes, T. E. (2015) Efficacy and safety of beloranib for weight loss in obese adults: A randomized controlled trial. *Diabetes Obes. Metab.* **17,** 566–572 CrossRef Medline
8. Hughes, T. E., Kim, D. D., Marjason, J., Proietto, J., Whitehead, J. P., and Vath, J. E. (2013) Ascending dose-controlled trial of beloranib, a novel obesity treatment for safety, tolerability, and weight loss in obese women. *Obesity* **21,** 1782–1788 CrossRef Medline
9. Betz, M. J., and Enerbäck, S. (2015) Human brown adipose tissue: What we have learned so far. *Diabetes* **64,** 2352–2360 CrossRef Medline
10. Wang, J., Sheppard, G. S., Lou, P., Kawai, M., BaMaung, N., Erickson, S. A., Tucker-Garcia, L., Park, C., Bouska, J., Wang, Y. C., Frost, D., Tapang, P., Albert, D. H., Morgan, S. J., Morowitz, M., Shusterman, S., Maris, J. M., Lesniewski, R., and Henkin, J. (2003) Tumor suppression by a rationally designed reversible inhibitor of methionine aminopeptidase-2. *Cancer Res.* **63,** 7861–7869 Medline
11. Towbin, H., Bair, K. W., DeCaprio, J. A., Eck, M. J., Kim, S., Kinder, F. R., Morollo, A., Mueller, D. R., Schindler, P., Song, H. K., van Oostrum, J., Versace, R. W., Voshol, H., Wood, J., Zabludoff, S., and Phillips, P. E. (2003) Proteomics-based target identification: Bengamides as a new class of methionine aminopeptidase inhibitors. *J. Biol. Chem.* **278,** 52964–52971 CrossRef Medline
12. Koves, T. R., Ussher, J. R., Noland, R. C., Slentz, D., Mosedale, M., Ilkayeva, O., Bain, J., Stevens, R., Dyck, J. R., Newgard, C. B., Lopaschuk, G. D., and Muoio, D. M. (2008) Mitochondrial overload and incomplete fatty acid oxidation contribute to skeletal muscle insulin resistance. *Cell Metab.* **7,** 45–56 CrossRef Medline
13. Yehuda-Shnaidman, E., Buehrer, B., Pi, J., Kumar, N., and Collins, S. (2010) Acute stimulation of white adipocyte respiration by PKA-induced lipolysis. *Diabetes* **59,** 2474–2483 CrossRef Medline
14. Reynisdottir, S., Wahrenberg, H., Carlström, K., Rössner, S., and Arner, P. (1994) Catecholamine resistance in fat cells of women with upper-body obesity due to decreased expression of beta 2-adrenoceptors. *Diabetologia* **37,** 428–435 CrossRef Medline
15. Jocken, J. W., and Blaak, E. E. (2008) Catecholamine-induced lipolysis in adipose tissue and skeletal muscle in obesity. *Physiol. Behav.* **94,** 219–230 CrossRef Medline
16. Horowitz, J. F., and Klein, S. (2000) Whole body and abdominal lipolytic sensitivity to epinephrine is suppressed in upper body obese women. *Am. J. Physiol. Endocrinol. Metab.* **278,** E1144–E1152 CrossRef Medline
17. Bougnères, P., Stunff, C. L., Pecqueur, C., Pinglier, E., Adnot, P., and Ricquier, D. (1997) In vivo resistance of lipolysis to epinephrine. A new fea-

ture of childhood onset obesity. *J. Clin. Invest.* **99,** 2568–2573 CrossRef Medline

18. Arner, P. (1999) Catecholamine-induced lipolysis in obesity. *Int. J. Obes. Relat. Metab. Disord.* **23,** Suppl. 1, 10–13 Medline
19. Bargut, T. C., Aguila, M. B., and Mandarim-de-Lacerda, C. A. (2016) Brown adipose tissue: Updates in cellular and molecular biology. *Tissue Cell* **48,** 452–460 CrossRef Medline
20. Zlobine, I., Gopal, K., and Ussher, J. R. (2016) Lipotoxicity in obesity and diabetes-related cardiac dysfunction. *Biochim. Biophys. Acta* **1861,** 1555–1568 CrossRef Medline
21. Chaurasia, B., Kaddai, V. A., Lancaster, G. I., Henstridge, D. C., Sriram, S., Galam, D. L. A., Gopalan, V., Prakash, K. N. B., Velan, S. S., Bulchand, S., Tsong, T. J., Wang, M., Siddique, M. M., Yuguang, G., Sigmundsson, K., *et al.* (2016) Adipocyte ceramides regulate subcutaneous adipose browning, inflammation, and metabolism. *Cell Metab.* **24,** 820–834 CrossRef Medline
22. Wanders, D., Burk, D. H., Cortez, C. C., Van, N. T., Stone, K. P., Baker, M., Mendoza, T., Mynatt, R. L., and Gettys, T. W. (2015) UCP1 is an essential mediator of the effects of methionine restriction on energy balance but not insulin sensitivity. *FASEB J.* **29,** 2603–2615 CrossRef Medline
23. Malloy, V. L., Krajcik, R. A., Bailey, S. J., Hristopoulos, G., Plummer, J. D., and Orentreich, N. (2006) Methionine restriction decreases visceral fat mass and preserves insulin action in aging male Fischer 344 rats independent of energy restriction. *Aging Cell* **5,** 305–314 CrossRef Medline
24. Hasek, B. E., Boudreau, A., Shin, J., Feng, D., Hulver, M., Van, N. T., Laque, A., Stewart, L. K., Stone, K. P., Wanders, D., Ghosh, S., Pessin, J. E., and Gettys, T. W. (2013) Remodeling the integration of lipid metabolism between liver and adipose tissue by dietary methionine restriction in rats. *Diabetes* **62,** 3362–3372 CrossRef Medline
25. Zhou, X., He, L., Wan, D., Yang, H., Yao, K., Wu, G., Wu, X., and Yin, Y. (2016) Methionine restriction on lipid metabolism and its possible mechanisms. *Amino Acids* **48,** 1533–1540 CrossRef Medline
26. Uhlén, M., Fagerberg, L., Hallström, B. M., Lindskog, C., Oksvold, P., Mardinoglu, A., Sivertsson, Å., Kampf, C., Sjöstedt, E., Asplund, A., Olsson, I., Edlund, K., Lundberg, E., Navani, S., Szigyarto, C. A., *et al.* (2015) Proteomics: Tissue-based map of the human proteome. *Science* **347,** 1260419 CrossRef Medline